2003227064

(2)

SEC

AD-A262 274

APR 1 1993

JMENTATION PAGE

Form Approved
OMB No. 0704-0188

IFIED	1b. RESTRICTIVE MARKINGS: N/A
2a. SECURITY CLASSIFICATION AUTHORITY	3. DISTRIBUTION/AVAILABILITY OF REPORT
2b. DECLASSIFICATION/DOWNGRADING SCHEDULE	Unlimited
4. PERFORMING ORGANIZATION REPORT NUMBER(S)	5. MONITORING ORGANIZATION REPORT NUMBER(S): AFOSR-TR- [illegible] 0179
6a. NAME OF PERFORMING ORGANIZATION: Indiana University	6b. OFFICE SYMBOL (If applicable):
6c. ADDRESS (City, State, and ZIP Code): 4601 Central Avenue, Columbus IN 47203	7a. NAME OF MONITORING ORGANIZATION: AFOSR
8a. NAME OF FUNDING/SPONSORING ORGANIZATION: AFOSR	8b. OFFICE SYMBOL (If applicable): NL
8c. ADDRESS (City, State, and ZIP Code): Building 410, Bolling AFB DC 20332-6448	7b. ADDRESS (City, State, and ZIP Code): Building 410, Bolling AFB DC 20332-6448
	9. PROCUREMENT INSTRUMENT IDENTIFICATION NUM: AFOSR-90-0126
	10. SOURCE OF FUNDING NUMBERS

PROGRAM ELEMENT NO.	PROJECT NO.	TASK NO	WORK UNIT ACCESSION NO.
61102F	2312	A5	

11. TITLE (Include Security Classification): The molecular anatomy of PFDA hepatotoxicity as studied by two-dimensional electrophoresis

12. PERSONAL AUTHOR(S): Frank A. Witzmann, Ph.D.

13a. TYPE OF REPORT	13b. TIME COVERED	14. DATE OF REPORT (Year, Month, Day)	15. PAGE COUNT
FINAL	FROM 15Dec89 - 14Dec92	26FEB93	23

16. SUPPLEMENTARY NOTATION

17. COSATI CODES		
FIELD	GROUP	SUB-GROUP

18. SUBJECT TERMS (Continue on reverse if necessary and identify by block number): rat liver; perfluoro-n-decanoic acid; hepatotoxicity; two-dimensional electrophoresis; peroxisome proliferation; image analysis

19. ABSTRACT (Continue on reverse if necessary and identify by block number)

Perfluoro-n-decanoic acid (PFDA) effects on protein expression in the rat liver were studied in rodents following in vivo exposure to PFDA levels above, below and at the LD-50. Two-dimensional whole-liver homogenate protein patterns were generated and compared to previous results. As before, numerous proteins were altered; some suppressed, some induced, but most were unaffected. In an effort to identify the altered proteins, further analysis of basic proteins by first-dimension NEPHGE revealed the induction of cytochrome P452 (lauric acid ω-oxidase) and enoyl-CoA hydratase. Induction of these and related enzymes confirms previously observed PFDA-induced peroxisome proliferation and lends strong support to the notion that PFDA blocks normal β-oxidation, causes fatty acid accumulation, and results in compensatory peroxisomal and mitochondrial ω- and β-oxidation. Continued identification of other altered proteins will be undertaken to add to the metabolic paths affected by PFDA to further delineate its toxic mechanism.

20. DISTRIBUTION/AVAILABILITY OF ABSTRACT	21. ABSTRACT SECURITY CLASSIFICATION
☐ UNCLASSIFIED/UNLIMITED ☐ SAME AS RPT ☐ DTIC USERS	Unclassified
22a. NAME OF RESPONSIBLE INDIVIDUAL: Dr. Walt Kozumbo	22b. TELEPHONE (Include Area Code): 202-767-5021 / 22c. OFFICE SYMBOL: NL

DD Form 1473, JUN 86 — Previous editions are obsolete — SECURITY CLASSIFICATION OF THIS PAGE

THE MOLECULAR ANATOMY OF PFDA HEPATOTOXICITY AS STUDIED BY TWO-DIMENSIONAL ELECTROPHORESIS

Frank A. Witzmann, Ph.D.
Department of Biology
Indiana University-Purdue University at Indianapolis
Columbus Campus
4601 Central Avenue
Columbus IN 47203

14 Jan 1993

Final Technical Report for Period 15 Dec 89 through 14 Dec 92

Prepared for:

Dr. Walt Kuzumbo
Directorate of Life Sciences
AFOSR
Building 410
Bolling AFB DC 20332-6448

INTRODUCTION

Within the last 20 years, technological developments in two-dimensional electrophoretic protein separation have made possible the resolution and comparison of complex mixtures of thousands of proteins from hundreds of samples (1-5). During the last 10 of those years, two-dimensional (2-D) protein electrophoresis has become a powerful tool in molecular biology and has found increasing application in pharmacologic and toxicologic investigations (5-15). The primary motivation behind developing this technique in toxicology has been the potential informational capabilities 2-D protein patterns provide regarding toxicologic phenomena. In this respect, one operates under the assumption that the comparative abundance and electrophoretic characteristics of cellular proteins are indicative of cell activities at the molecular level. By describing the changes observed in the pattern of protein expression, *i.e.* drug/chemical-induced abnormality, we endeavor to *1)* describe and understand, from a uniquely informative perspective, specific xenobiotic effects and *2)* predict others on the basis of structure-activity relationships.

The present project addressed the feasibilty of analyzing rodent hepatotoxicity by examining the protein patterns of rat liver whole homogenates and cell fractions generated by large-scale (2-3) 2-D electrophoresis. Our intent was to evaluate the utility of this approach in toxicity testing by generating 2D liver protein patterns representing various levels of intoxication with the assumption that changes in hepatocellular protein expression are specific indicators of cell injury and dysfunction. The compound chosen initially, perfluoro-n-decanoic acid (PFDA), is a ten carbon straight-chain perfluorinated carboxylic acid whose surfactant properties give it and chemically similar compounds important commercial application. Substantial previous investigation of PFDA's hepatotoxicity has demonstrated that a single 50mg/kg i.p. dose (16) induces significant weight loss characterized by hypophagia (17, hepatomegaly, peroxisome proliferation (18-20), and delayed lethality in rats. More recent observations have led to the notion that PFDA interferes with normal β-oxidation of fatty acids resulting in an accumulation of fatty acids in the cell (21). As a result of this accumulation, peroxisomes proliferate as a prominent feature of compensatory β- (22,23) and ω-oxidative inductions (24,25). Accordingly, a broad base of hepatotoxicologic phenomena associated with perfluorocarboxylic acid toxicity are available for comparison with molecular changes in the form of 2-D protein pattern alterations.

Presented in this report are the final results of this three-year investigation, some of which have been reported to AFOSR via Annual Technical Reports as well as published and/or presented at scientific meetings (26-34). It is important to note that the results reflect a natural progression in quality and technique as innovative technological developments, *i.e.* ours (30) and others, were incorporated into our protocols. Electrophoretic data will be presented which confirm previous systemic observations regarding PFDA's hepatotoxicity mentioned above.

From the same data it will be clear that although it is a potent peroxisome proliferator, PFDA exerts its cellular effects differently when compared to other structurally diverse peroxisome proliferators.

Additional data that document the value of large-scale, high-resolution 2-D electrophoresis and computerized image analysis in relating molecular changes to xenobiotic effects are also included in this report. This evidence will illustrate that we are meeting the following previously established criteria (13) for systematic use of 2-D electrophoresis in toxicology: *1)* a useful range of known effects produces detectable changes at the molecular level, *2)* that there is sufficient specificity associated with molecular effects to differentiate various classes of mechanisms, and *3)* that there is some basis for expecting that the molecular changes can be interpreted in a way that helps illuminate not only the details, but also the possible significance, of the events observed.

TECHNICAL APPROACH

Animal Care and Intoxication

Male Fisher-344 rats (225-250g) were obtained from Charles River Breeding Labs, individually housed, and maintained on rat chow and water *ad libitum*. Rats were injected intraperitonealy with either of the following:

2mg, 20mg or 50mg **PFDA**/kg body weight; single injection; animals sacrificed on day 8 of exposure

150mg **PFOA**/kg (perfluorooctanoate, PFDA's eight carbon analog); single injection; animals sacrificed on day 3 of exposure

250mg **clofibrate**/kg; single injection on each of 3 successive days; animals sacrificed on day five of exposure

1200mg **DEHP**/kg (di[2-ethylhexyl]phthalate); single injection on each of 3 successive days; animals sacrificed on day 5 of exposure

1.25g/kg **polyCTFE** (chlorotrifluoroethylene); daily injection on each of 7 successive days; rats sacrificed on day 8 of exposure

Matched control rats were vehicle injected and pair fed (PFC)

Sample Preparation

After the appropriate exposure period, livers were surgically removed from the ketamine/xylazine anesthetized rats and manually perfused with ice-cold saline to remove excess blood. One 0.5g piece was removed, minced, and homogenized in 8 volumes (4mL) of a lysis buffer containing 9M urea, 4% NP-40, 2% DTE (dithioerythritol), and 2% ampholytes (Serva pH 9-11) pH 9.5 for ISO-DALT® electrophoresis (35). A second piece of liver tissue was minced and homogenized in ice-cold 0.25M sucrose. Microsomal and mitochondrial fractions were prepared from this homogenate by differential centrifugation (36). These fractions were

then solubilized in either a lysis buffer containing 9M urea, 4% dodecyl-maltoside detergent, [and later 2% NP-40 and 2% dodecyl-maltoside detergents], 2% β-mercaptoethanol, 2% ampholyte (Serva pH 2-11) at pH 3.0 (35) for nonequilibrium pH-gradient electrophoresis *(NEPHGE-DALT)* or the lysis buffer described above for conventional ISO-DALT® runs. After complete solubilization at room temperature for 120min, all samples were centrifuged at 110,000 x *g* using a Beckman TL-100 ultracentrifuge and stored at -70°C.

Two-dimensional Electrophoresis (conventional)

The strength of the 2-D electrophoretic technique lies in its ability to resolve literally thousands of cellular proteins first based on their content of acidic and basic amino acids **(isoelectric focusing)** and second by molecular weight **(SDS electrophoresis)**. In combination, these two separation techniques produce a two dimensional protein pattern unique for a specific group of cells/tissues. Individual proteins within the pattern can be analyzed for alterations in volume (density), charge, and (least likely) molecular weight. Changes in volume or spot density reflect alterations in a protein's abundance and suggest up- or down-regulation of the genome or altered protein turnover rates. Charge modifications suggest either posttranslational modification alterations or point mutations in the genome.

Using the Anderson ISO-DALT® (2-D Electrophoresis) System (35), 10μL of the solubilized protein sample was placed on each of 20 first dimension gels (25cm x 1.5mm) containing 4% acrylamide, 2% NP-40, 2% ampholyte (BDH pH 4-8) and electrophoresed for 32,000 VHr at room emperature. Each first dimension gel was then placed on a second-dimension DALT slab gel (20cm x 25cm x 1.5mm) containing a linear 9-17% acrylamide gradient. During initial phases of the investigation these gradient slab gels were manually poured as described (35) using the ISO-DALT® 300 DALT gradient maker (Hoefer Sci). Later in the investigation gradient slab gels were poured more easily and reproducibly using the ANGELIQUE™ computer-controlled gradient maker (Large Scale Biology Corp.). This system enables one to reduce run-to-run variability in the polyacrylamide gel concentration, an essential characteristic for protein pattern image analysis. Molecular weight standards were comigrated on the gel margin while internal charge standardization of was accomplished using carbamylated creatine kinase charge-train standards. DALT gels were run for 18hr at 4°C and later stained with Coommassie brilliant blue G-250 (37). Protein patterns on some gels were electroblotted onto nitrocellulose for immunological identification of specific proteins. Initially, all stained gels and protein blots were photographed on a fluorescent light box with Kodak Panatomic-X film and printed on Ilford Multigrade III photographic paper for both visual analysis of protein spot patterns as well as archiving. After recently acquiring imaging technology, stained gels and protein blots were processed and archived as described later. Polyclonal antibodies were the generous gifts of the following: anti-cytP452 (cytochrome P450IVA) and anti-trifunctional enzyme (enoyl-CoA hydratase) from G.G. Gibson, Univ. of Surrey; anti-FABP (fatty acid binding protein) from J. Vanden Heuvel, Univ. of Wisconsin, Madison; anti-TFA (trifluoroacetylated) protein from L. Pohl, NIH.

Two-dimensional Electrophoresis (Nonequilibrium pH-Gradient Electrophoresis [NEPHGE] in the first dimension)

Despite their proven utility, conventional 2-D techniques have inherent difficulty in generating isoelectric focusing gradients at extremes of pH with broad range ampholytes, proving especially unstable at alkaline pH. Consequently, proteins with alkaline pI's such as the cytochromes P450 and other important enzymes altered by PFDA toxicity were poorly resolved in our conventional system. One approach to visualizing basic proteins has been to run NEPHGE (38) gels in the first dimension followed by conventional SDS-PAGE in the second. To identify very basic proteins altered in rat liver cell fractions by perfluorochemical intoxication we used the NEPHGE-DALT approach (30). 2-D electrophoresis was conducted using rat liver mitochondria and microsomes solubilized in a lysis buffer containing 9 M urea, 2% (v/v) β-mercaptoethanol, 2% (v/v) ampholytes (BDH pH 3.5-10) and *either* 4% (v/v) NP-40 detergent *or* 4% dodecyl maltoside detergent at a final pH of 3.0. Forty microliters of sample (approximately 400μg protein) was placed on each of 20 ISO tubes containing 4% acrylamide, 2% NP-40, 9 M urea, and 5% ampholyte (BDH, pH 3.5-10) and first-dimension tube-gels run for 4000 V·hr. Following NEPHGE, tube-gels were immediately placed on each of 20 DALT gels containing a linear 9-17% acrylamide gradient along with molecular weight standards along the gel margin and run via conventional DALT protocol.

Image Analysis

Stained gels were digitized at 125 micron resolution using an Ektron 1412 CCD scanner that produces 8 bit images in the optical density domain with up to 2048x2048 pixels although most images were 1800x2000 pixels on a side. The gel images were processed on a DEC VAXStation 3100 M76 workstation using the KEPLER® software system (Large Scale Biology Corp.) with procedure PROC008 which includes background and streak subtraction, erosion/dilation spot cutout, and 2-D Gaussian fitting to generate a spotlist giving *x,y* position, shape, and density information for each detected spot. Groups of numerous sample gels corresponding to all the animal treatment groups were assembled and matched to a standard master pattern for that particular experiment and set of running conditions. This master pattern was initially constructed from a representative clone and additional spots added that were detected in other gel image clones to develop a master pattern containing all detectable protein spots. Individual gel patterns were scaled together using a linear fit to the abundances of selected matched spots to compensate for variations in sample protein loading. Groupwise statistical comparisons (Student's t-Test, Product Moment Correlation Coefficient, etc.) were made graphically and interactively and the results displayed in montage format using the KPL42 module. Graphical results were printed on a microLaser Plus printer (Texas Instr.) while raw gel images, processed images, and montages were printed using a 64 level grey-scale videoprinter (Codonics).

RESULTS AND DISCUSSION

NEPHGE-DALT Electrophoresis

Figure 1 illustrates the rat liver mitochondrial fraction NEPHGE-DALT patterns obtained using the two different detergents. Clearly, dodecyl maltoside solubilized proteins formed more discreet spots and migrated farther under the nonequilibrium conditions when compared to those solubilized with NP-40. Subsequent experiments (not shown) demonstrated that a 50/50 mixture of the two detergents resolved the proteins more reproducibly than dodecyl

maltoside alone. Consequently, all NEPHGE first-dimension runs now incorporate this nonionic detergent.

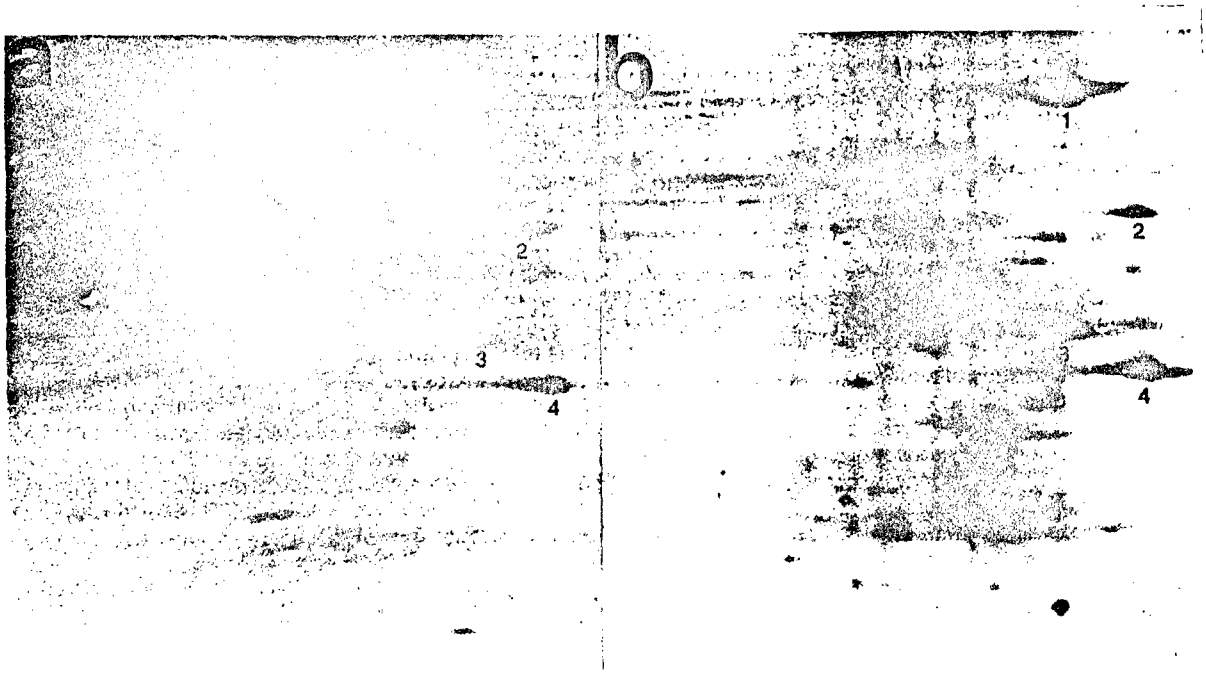

Figure 1. 2-D PAGE (NEPHGE-DALT) of liver mitochondrial fraction from a rat treated with a peroxisome inducer, perfluoro-*n*-decanoic acid. 400 µg of protein was loaded and gels stained with Coomassie Brilliant Blue G-250. The 2-D pattern in (A) was generated from proteins solubilized in NP-40 detergent while panel (B) illustrates dodecyl maltoside solubilization. Proteins labeled 1, 3, and 4 are peroxisomal enoyl CoA hydratase (bifunctional enzyme; 78 kDa) and its constituent polypeptides (39.5 and 35.1 kDa). Protein 2 is cytochrome P450IVA1 (lauric acid ω-oxidase; 52.5 kDa).

PFDA exposure described above was associated with significant alterations of the 2D protein pattern in the mitochondrial fraction (Figure 2) tested. PFOA's effect on pattern alteration was similar to PFDA's but less intense. Clofibrate also showed some similarities although compartmental differences in its effect were notable. Foremost among the alterations observed were those illustrated in Figure 2 (panels I-VI). In NEPHGE-DALT separation of the mitochondrial fraction, several proteins with alkaline pI's were induced relative to dose, xenobiote, and cellular compartment. Catalase (diamond-shaped box) was identified by coomigration of the purified form. With the exception of the thiolase, the following were identified immunologically on protein blots of replicate gels: (A) peroxisomal/microsomal enoyl-CoA hydratase (bifunctional enzyme; (B) cytochrome P45IVA1 [cyt P452] (lauric acid ω-oxidase); (C) peroxisomal enoyl-CoA hydratase polypeptide I; (D) peroxisomal enoyl-CoA hydratase polypeptide II; (E) 3-ketoacyl-CoA thiolase and (F) mitochondrial enoyl-CoA hydratase (crotonase) represent the most notable inductions. Panels I-IV represent replicate sample gels from the following treatments: (I) control; (II) 50mg/kg PFDA; (III) 100mg/kg PFOA; and (IV) 400mg/kg clofibrate. Panels V and VI are nitrocellulose blots of PFDA-treated patterns exposed to polyclonal antibodies raised against purified rat hepatic bifunctional enzyme (enoyl

CoA-hydratase). Panel (V) illustrates the microsomal pattern (note absence of the mitochondrial protein F, crotonase). Panel (VI) illustrates the mitochondrial pattern.

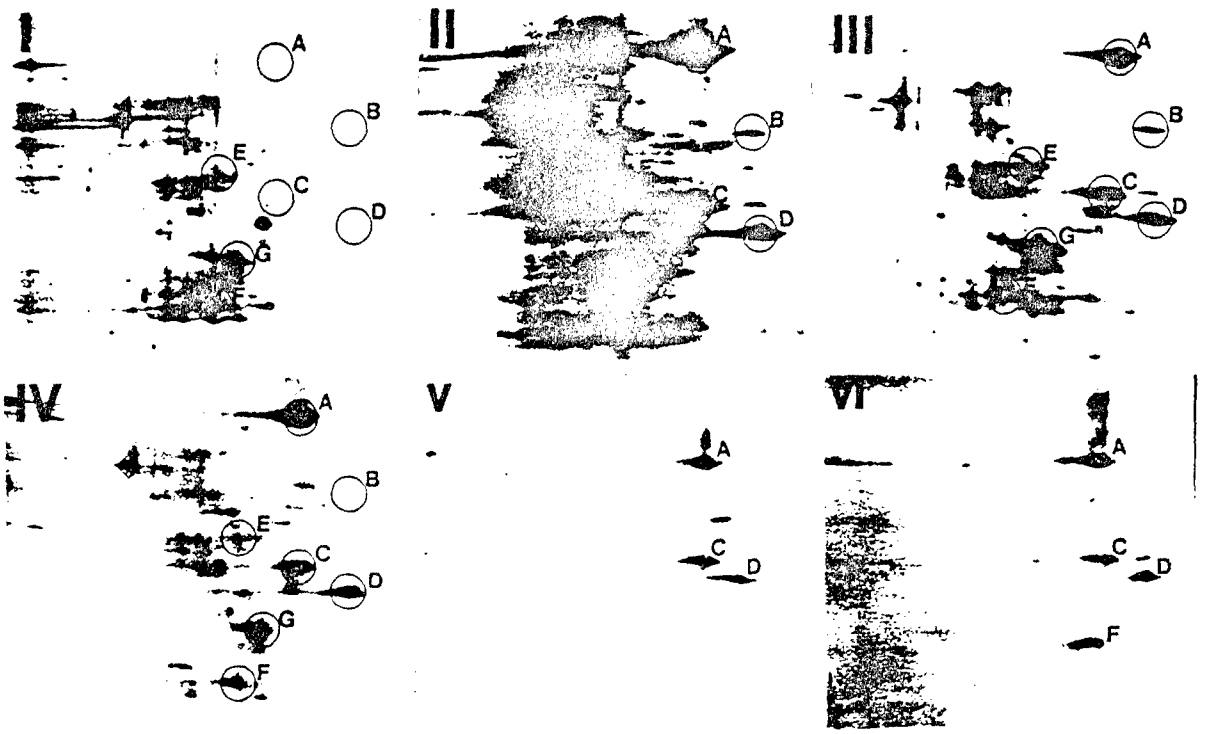

Figure 2. Rat liver mitochondrial fraction, proteins separated by NEPHGE in the first-dimension. Proteins appearing on these gels have very basic pI's and consequently do not appear on conventional ISO-DALT patterns. Significant induction of peroxisomal β-oxidative enzymes by xenobiotic treatment is shown. Individual panels are described in the text above.

ISO-DALT Electrophoresis

Microsomal fractions separated by conventional 2D-PAGE are illustrated in Figure 4. Each panel represents replicate gels of several samples from (5) control; (6) 50mg/kg PFDA-exposed; (7) 7 daily 1.25g/kg polyCTFE doses; and (8) 400 mg/kg clofibrate treated. The encircled charge train resembles the ~78 kDa hepatic protein previously shown to be trifluoroacetylated [39]. A minor but readily apparent alteration in the composition of that spot-group is induced by PFDA exposure, but not by polyCTFE nor clofibrate. The nature of this apparent charge shift in the train of proteins suggests protein acylation by PFDA.

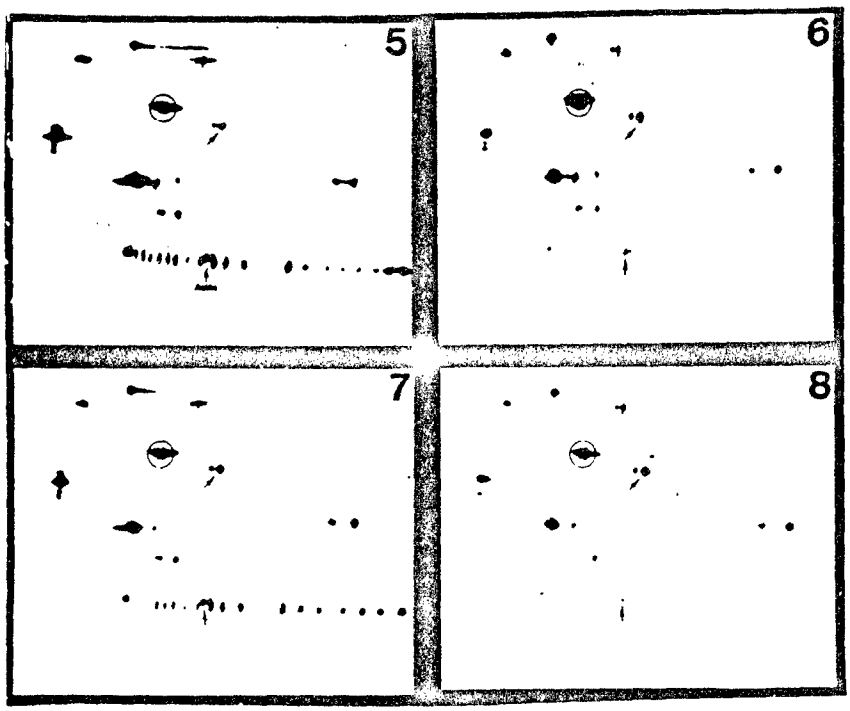

Figure 3. Rat liver microsomal protein patterns generated by conventional ISO-DALT procedures. (5) control, (6) PFDA 50mg/kg PFDA exposed, (7) CTFE exposed, and (8) clofibrate-treated. Creatine kinase carbamylated charge standards shown in panels 5 and 7. Only panel 6 exhibits charge modification of encircled protein charge train.

More recent experiments incorporating the Kepler System have generated a 2D protein map for rat liver and eneabled us to investigate, in greater detail, the observation above as well as several other previously observed protein pattern alterations. Figure 4 on the following page illustrates a two-dimensional protein map generated by the Kepler System for rat liver whole homogenates. By convention, isoelectrically focused proteins (horizontal dimension) are oriented with acidic proteins toward the left and basic proteins toward the right. High molecular weight proteins are located near the top of the pattern while lower molecular weight proteins migrate toward the bottom. The pattern in Fig. 4 is essentially a composite of more than 1400 proteins found in sample patterns and is used to match sample patterns and illustrate pattern alterations. Highlighted spots (opaque) represent those proteins whose identity has been ascertained with high probability.

Each spot (polypeptide) in the pattern represents numerical data regarding coordinate position and density. In contrast to our previous reliance on black and white photographs to analyze protein alterations, we are now able to observe positional and integrated density variations in over 800 matched protein spots and statistically determine the significance of their alteration.

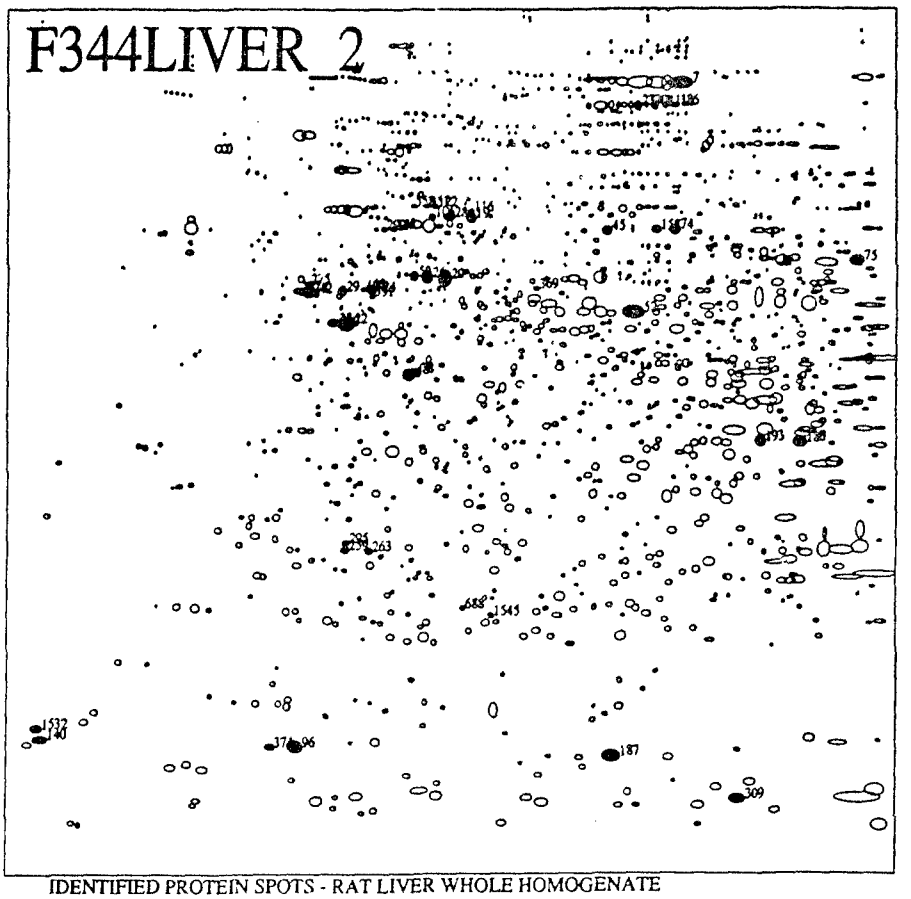

Figure 4. Schematic representation of the 2D electrophoretic standard master pattern map of F344 rat liver whole homogenate proteins. Each detected protein is represented as a circle or an elipse with those conclusively identified filled in black (see Table 1). Susequent figures and data are generated by similar mapping techniques.

Table 1, found on pages 10-11, lists the identified proteins highlighted on the map in Figure 4 along with their database identification, estimated molecular weight, x and y coordinate position (in the master number system F344LIVER), and integrated density of each protein as it appears in normal, control rat livers. Those proteins found only in experimentai groups but included in the master pattern are listed as well.

TABLE 1. HEPATIC PROTEINS IDENTIFIED BY 2D-PAGE (F344LIVER_1 MASTER SYSTEM)

PROTEIN NAME	KPL_ID	MSN	MW	X	Y	VOL
actin-β	ACTIN_BETA	48	43.8	1406.3	1118.1	110,316
actin-γ	ACTIN_GAMMA	78	43.9	1433.5	1114.9	33,464
albumin	ALBUMIN	45	62.3	2974.9	680.1	38,444
3-α-hydroxysteroid-dihydrodiol-dehydrogenase	3_ALPHA_HDDH	180	37.7	2772.8	1326.9	94,776
		193	37.8	2630.0	1323.2	55,111
apo A-I plasma lipoprotein	APO_A-I	688	25.8	1594.6	1826.1	4,585
		1545	25.4	1693.7	1847.8	5,089
calmodulin	CALMODULIN	140	15.3	117.1	2247.6	32,086
		1532	16.2	103.7	2190.9	17,929
carbamoyl-phosphate synthase	CPS	7	160.1	2347.0	233.7	168,841
catalase	CATALASE	75	56.9	2974.9	772.8	71,890
cytochrome b_5	CYTOCHROME_B5	96	17.4	1009.8	2223.7	118,652
		374	17.4	922.8	2247.6	11,019
enoyl-CoA hydratase (mitochondrial)	*	*	26.8	*	*	*
enoyl-CoA hydratase (peroxisomal)	*	*	78	*	*	*
enoyl-CoA hydratase subunit I (perox.)	*	*	39.5	*	*	*
enoyl-CoA hydratase subunit II (perox.)	*	*	35.1	*	*	*
F1 ATPase, β subunit (mitochondrial)	MITCON:1	22	50.0	1183.9	959.6	207,873
	MITCON:1	33	50.1	1139.2	958.4	44,881
fatty acid binding protein (FABP)	FABP-L	309	13.6	2552.5	2409.4	67,162
3-OH-3-methylglutaryl CoA synthase (mito.)	HMG_COA_SYNTHASE	259	29.7	1179.7	1648.3	13,247
		263	29.8	1263.3	1652.2	13,898
		295	30.3	1183.2	1627.8	11,953
		369	53.7	1849.4	855.5	6,017
		558	69.1	1418.3	607.0	2,640
3-ketoacyl-CoA thiolase	*	*	44.5	*	*	*
lamin b	LAMIN_B	185	64.9	1352.4	673.9	6,805
		299	64.6	1318.6	675.7	4,853
lauric acid ω-oxidase (cyt P450IVA1)	*	*	52.5	*	*	*
mitcon:2 (HSP58)	MITCON:2	20	55.2	1527.9	825.5	162,660
		26	55.5	1465.5	821.1	85,907
		50	55.5	1419.5	818.1	24,367

*KPL_ID = Kepler identification label; MSN = master spot number (label); MW = estimated SDS molecular weight (kDaltons); X = x axis coordinate position; Y = y axis coordinate position; VOL = 6.28(δx)(δy), integrated density; * = proteins appear only on NEPHGE-DALT gels, pI>8.0.*

TABLE 1. HEPATIC PROTEINS IDENTIFIED BY 2D-PAGE (cont'd)

PROTEIN NAME	KPL_ID	MSN	MW	X	Y	VOL
mitcon:3 (GRP75)	MITCON:3	19	66.3	1523.4	640.8	61,639
		28	66.6	1547.5	639.3	33,843
		106	66.8	1486.1	637.8	10,550
		116	68.0	1623.2	621.0	9,819
NADPH cytochrome P450 reductase	NADPH_P450_RED	122	69.3	1494.8	606.9	8,211
		351	69.5	1467.1	607.0	4,292
protein disulfide isomerase 1	PDI	15	54.5	1053.6	864.3	90,756
		42	54.7	1077.5	867.5	25,932
		40	54.9	1030.2	863.2	25,360
		112	55.1	1014.5	861.5	11,220
		275	55.7	1048.4	840.6	5,678
pro-albumin	PRO-ALBUMIN	74	62.3	2327.9	677.3	45,648
		158	62.3	2262.2	677.7	19,015
pyruvate carboxylase	PYRUVATE_CARBOX	27	124.7	2202.3	302.6	27,032
		43	125.1	2258.9	302.5	20,898
		111	124.9	2297.0	301.1	9,862
		186	124.9	2337.3	300.6	7,053
		330	125.2	2229.8	301.2	4,551
stearoyl-CoA desaturase	STEAR_COA_DESAT	62	37.3	1346.0	1352.5	93,432
		141	37.3	1256.6	1353.0	20,275
superoxide dismutase	SOD	187	16.8	2122.7	2278.6	144,584
trifluoroacetylated protein (TFA)	TFA	5	67.9	1214.3	620.0	60,123
		14	68.4	1189.5	617.2	48,175
		18	68.8	1167.3	615.1	24,802
		1536	69.1	1142.2	613.4	12,869
		1537	69.4	1119.7	611.9	5,342
α tubulin	TUBULIN_ALPHA	60	54.4	1264.1	855.2	19,482
		124	54.1	1279.0	863.3	11,294
		391	53.6	1275.0	876.7	4,762
		494	53.8	1244.0	857.4	3,566
β tubulin	TUBULIN_BETA	29	53.9	1170.0	862.2	39,191
		103	53.4	1160.2	876.0	12,366

KPL_ID = Kepler identification label; MSN = master spot number (label); MW = estimated SDS molecular weight (kDaltons); X = x axis coordinate position; Y = y axis coordinate position; VOL = 6.28(δx)(δy), integrated density

Whereas much of our effort during the funded research period was focused on rat liver protein expression with respect to PFDA and related chemical exposures as part of our stated objectives, we also began prelimary investigation of liver protein patterns in other species. Using the Translation Table Utility provided by the Kepler Image Anlysis System, we intend to develop a comparative approach to our overall experimental strategy. This will expedite the application of this technique to *in vitro* toxicologic methodologies and improve extrapolation to man. To this end, presented in Figure 5 are preliminary 2D electrophoretic maps of guinea pig, baboon, and human liver whole homogenate proteins.

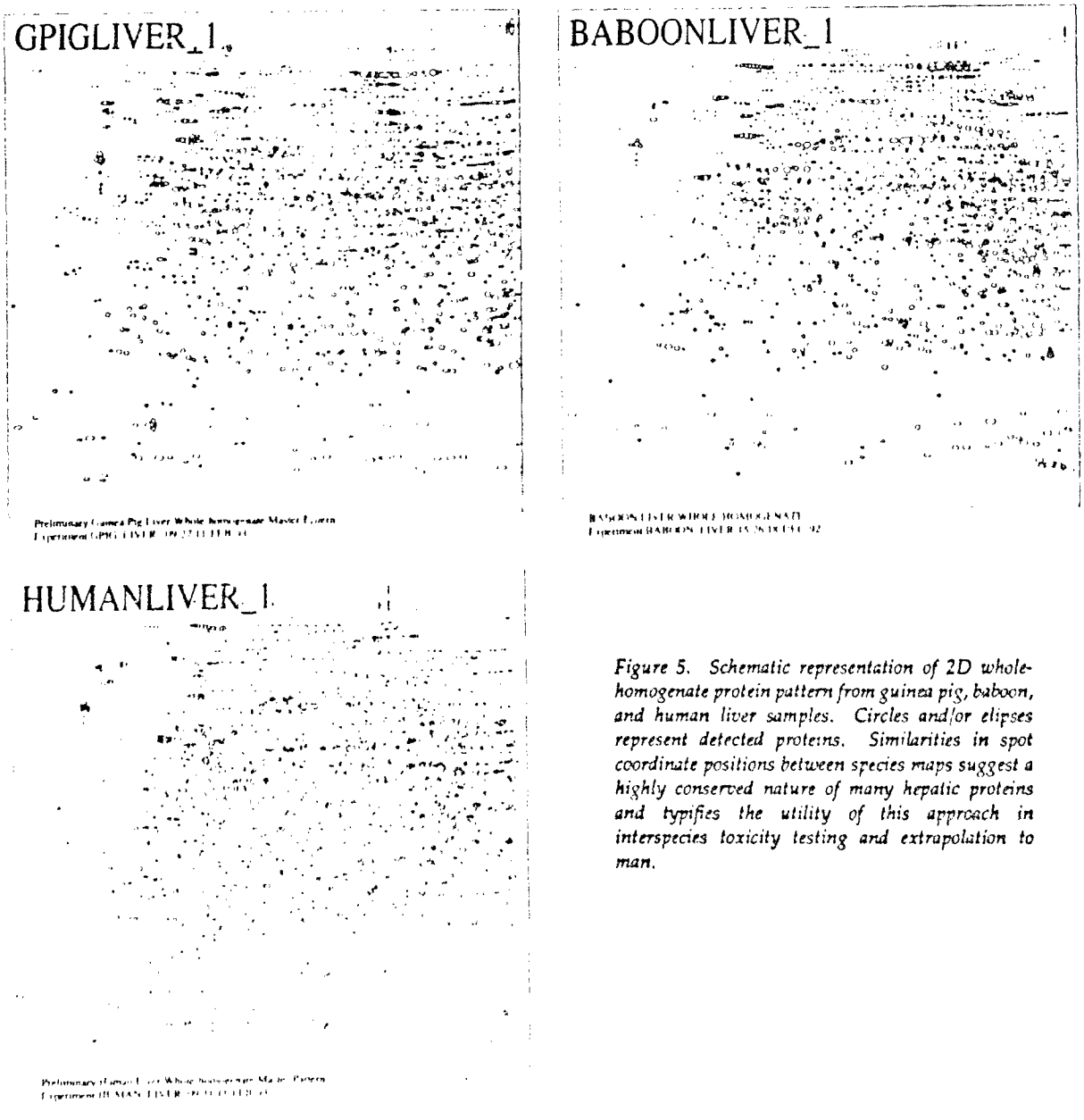

Figure 5. Schematic representation of 2D whole-homogenate protein pattern from guinea pig, baboon, and human liver samples. Circles and/or elipses represent detected proteins. Similarities in spot coordinate positions between species maps suggest a highly conserved nature of many hepatic proteins and typifies the utility of this approach in interspecies toxicity testing and extrapolation to man.

To assess the effect of the various exposures listed earlier, individual sample patterns were matched against the master pattern F344LIVER and variations in integrated spot density calculated via Student's paired t-test. Proteins that underwent significant, P<.001, alteration as a result of any or all treatments were highlighted in the master pattern for that group. In the nine groups tested, 86 total proteins across 8 experimental groups were altered by xenobiotic exposure and are shown below (Table 2 and Figure 6):

TABLE 2

TREATMENT (n)		NUMBER OF PROTEINS ALTERED (P<.001)
Pair-fed	(9)	2
PFOA (150mg/kg)	(8)	5
PFDA (2mg/kg)	(5)	1
PFDA (20mg/kg)	(5)	14
PFDA (50mg/kg; 8da)	(9)	63
PFDA (50mg/kg; 30da)	(5)	25
Clofibrate (250mg/kg)	(10)	6
DEHP (1.2mg)	(3)	4

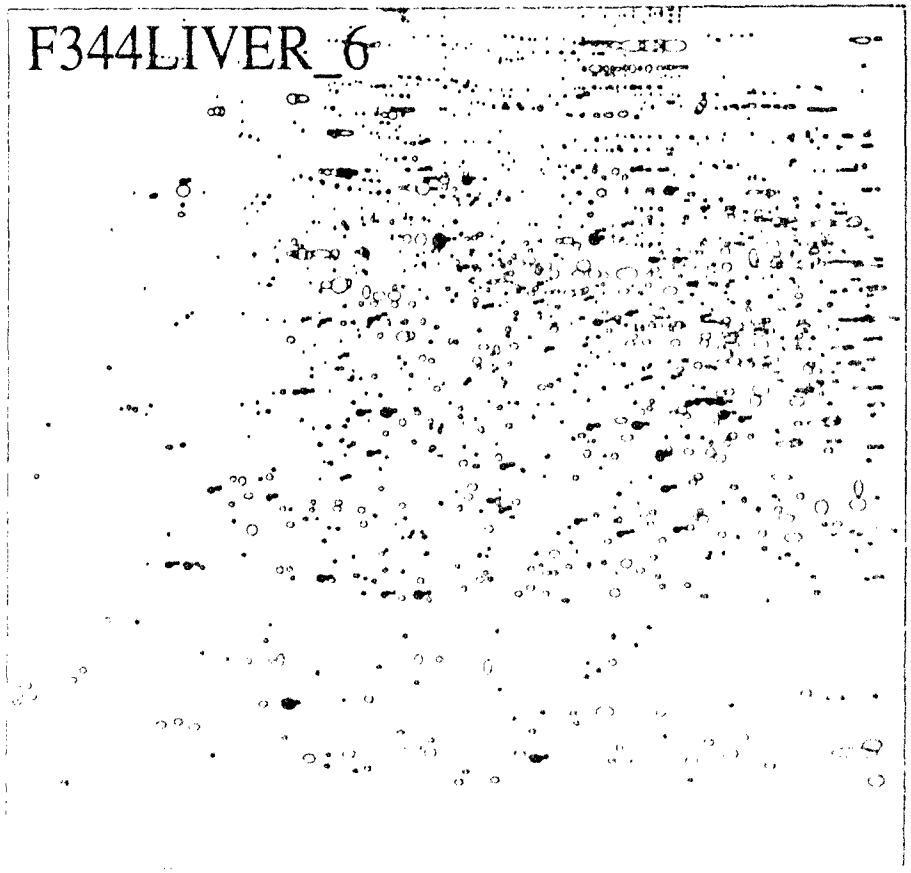

Figure 6. 2D protein map of rat liver whole homogenate proteins. This master pattern illustrates those proteins altered (1) by PFDA (P<.001) 8 days after a single 50mg/kg dose.

To visualize the treatment effects on the individual proteins in each sample by group, we have plotted the relative densities of each altered protein (P<.001). These are shown below in Figure 7. The abundance of each protein is displayed by master spot number (MSN) according to group. Using this plotting technique it is possible to observe conspicuous trends in the data. Furthermore, the relationship between individual proteins whose alteration trends are similar (i.e. MSN 5,36,62,96,113 [down-regulation with PFDA] or MSN 14,19.190,200 [up-regulation]) can be determined by calculation of the Pearson product-moment correlation coefficient.

Figure 7. This bar graph illustrates the proteins by master spot number (MSN), whose abundance has been altered by one or more of the eight treatments vs. control. Each box represents one protein with the MSN indicated. Individual bars represent the relative abundance of each protein indicated by bar height. The horizontal axis of each box is divided into the 9 groups in the following order: control, pair-fed, PFOA, PFDA 2mg/kg, PFDA 10mg/kg, PFDA 50mg/kg 8da, PFDA 50mg/kg 30da, Clofibrate, and DEHP.

Of the numerous proteins altered by xenobiotic treatment, several have recently been examined for group comparisons by one-way ANOVA and Student-Neuman-Keuls *post hoc* pairwise multiple comparisons and are presented below.

One of the unique features of PFDA toxicity observed previously *[20]* is the virtual abolition of stearoyl-CoA desaturase activity by both PFDA exposure and pair-feeding for 14 days in rodents. As Figure 8 illustrates, statistical analysis of integrated density of MSN62 (tentatively identified as stearoyl-CoA desaturase) by one-way ANOVA followed by Student-Newman-Keul *post hoc* test ($P<.05$) provides confirming electrophoretic evidence that the decline in enzyme activity is a result of decreased protein abundance after 8 days of PFDA exposure or pair-feeding. The data also illustrate that the PFDA effect persists even four weeks following a single exposure. Furthermore, it is clear that PFDA, in the single 2mg/kg exposure, has no significant effect on the abundance of this enzyme while increased exposure levels cause profound down-regulation. Structurally diverse PFOA, clofibrate, and DEHP, potent peroxisome proliferators, have a moderate effect in this regard.

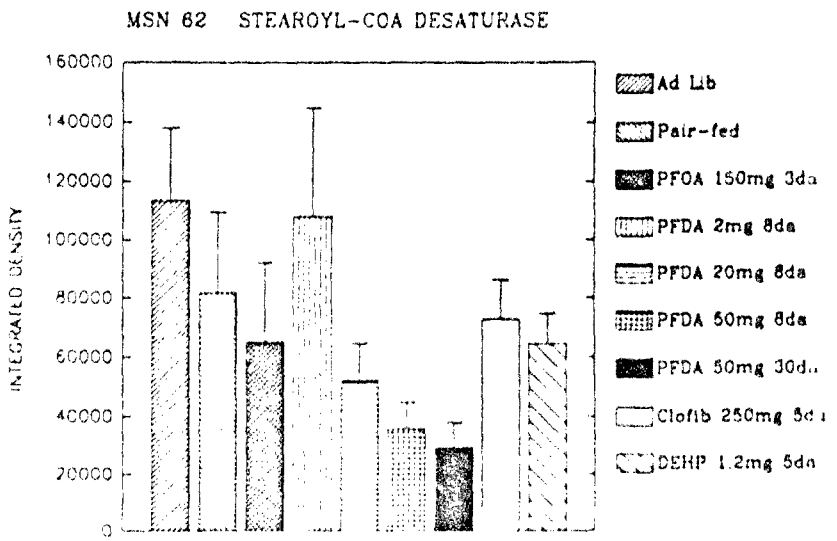

Figure 8. Effect of xenobiotic exposure on protein abundance as calculated by integrated density. $F=11.178$, $P<.001$. Values are mean ± SEM.

Similar statistical methodology was applied to three other identified protein spots whose mean integrated densities were altered by treatment. A significant reduction in rat liver cytochrome b_5 content as a result of PFDA exposure has also been observed previously [20]. Once again, Figure 9 (top) provides electrophoretic confirmation of assay data. In Fig. 9, only PFDA exposure of 50mg/kg (8 and 30 days) is associated with a significant reduction in the abundance of cyt b_5. The decline in cytochrome b_5 abundance (confirmed on 2D patterns of microsomal proteins, not shown) is particularly interesting in view of its role as the primary electron transfer protein in the desaturase reaction. The data further suggest that PFDA exposure results in significant reduction in electron transfer during cytochrome P450 catalyzed monoxygenations, for which b_5 is partly responsible. This may be related to the yet unconfirmed minor decline observed in NADPH-cytochrome P450 reductase (F344LIVER MSN

122 and 351), the major electron transfer protein to cytochromes P450. The relationship between these specific protein alterations to PFDA's toxic mechanism remains to be explained. Corregulation of spots as indicated by 2D results suggests that the spots are common to some tightly regulated biochemical pathway (as may be the case above), they are subunits of multimeric protein(s), or they are individaul components of vast cellular xenobiotic effects.

Figure 9 (middle) also illustrates the response of a mitochondrial stress protein Hsp58. This protein has been identified based on its homologous position in other mammalian systems [5] and is induced by heat shock, can be phosphorylated, and is also classified as a chaperonin (cpn60). Its induction (Fig. 9) by PFOA and PFDA is indicative of a stress response, perhaps oxidative stress. However, because the abundance of superoxide dismutase (SOD), a biomarker of oxidative stress (that converts free-radical O_2 to H_2O_2) and a difficult enzyme to assay, is significantly reduced by high-level PFDA exposure (Figure 9 - bottom), it is unlikely that PFDA is associated with classic oxidative stress. Instead, the H_2O_2 generated by the high levels of peroxisomal β-oxidative enzymes induced by PFDA [29,33] may cause feedback down-regulation of SOD synthesis. These three preliminary observations demonstrate the utility of this 2D electrophoretic approach and provide precursory information regarding the assorted effects these structurally diverse peroxisome proliferators have on the liver. These data also support the notion that peroxisome proliferators can be quite dissimilar mechanistically.

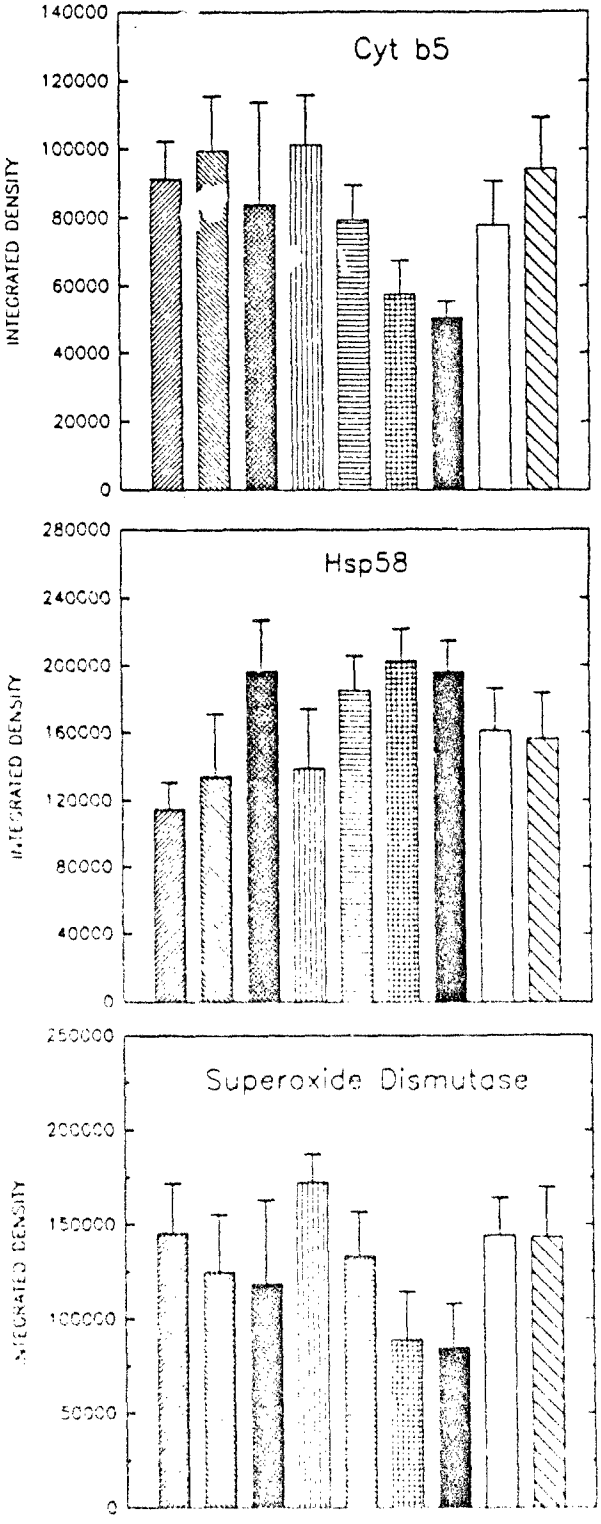

Figure 9. Integrated spot density group means ± SEM for three identified proteins: cytochrome b_5 (top), heat shock protein Hsp58 (chaperonin Cpn60) (middle), and superoxide dismutase (bottom). For group identification, see legend in Fig. 8 on previous page.

The separation characterization, and analysis of many membrane-associated proteins is particularly suited to 2D electrophoresis. Because many of these proteins are post-translationally modified (such as glycoproteins or phosphoproteins) they often exist as heterogeneous species with multiple isoelectric points. On a one-dimensional gel, these proteins appear as one large band. On 2D gels, these proteins exist as charge trains, with the native form having the most alkaline pI. We have examined a significant number of these heterogeneous proteins appearing in our liver patterns but have concentrated on a particular hepatic microsomal protein referred to as TFA protein (trifluoroacetylated) and tentatively identified as grp78 (glucose-regulated protein) or BiP, a member of the hsp70 family located on the endoplasmic reticulum. We have immunologically identified this protein in whole homogenate and microsomal fractions as the protein trifluoroacetylated following halothane anesthesia [39,40]. The 2D pattern of this protein is shown below in Figure 10.

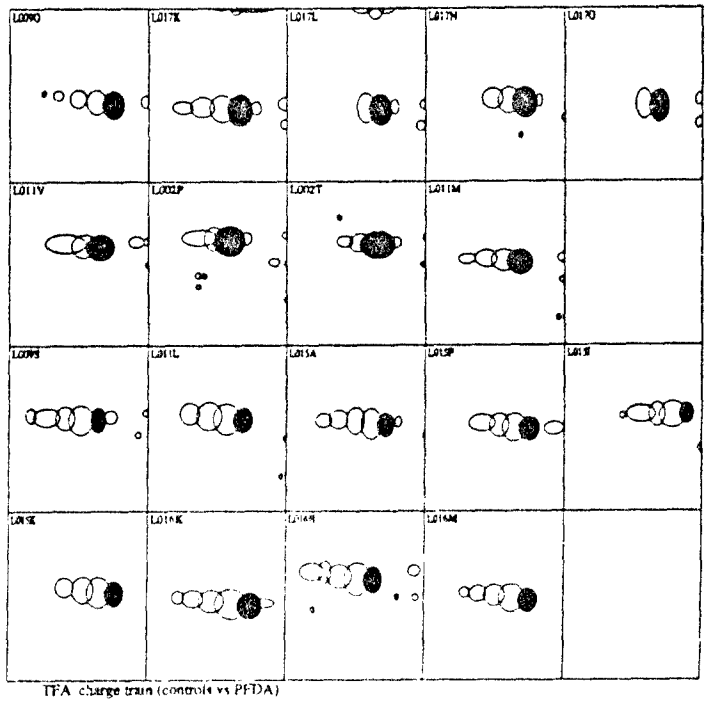

Figure 10. Montage showing the effects of PFDA intoxication on the expression of TFA protein in the same gel region of 18 different sample patterns. The first two horizontal rows are controls while the bottom two rows are PFDA-treated. The right-most spot (filled-in) in each charge train is MSN5 and represents the most abundant spot of any in the train. The remaining spots, in a leftward (acidic) direction are MSN14, 18, 1536, and 1537 (see Table 1, page 11). PFDA-treated livers undergo a significant leftward charge shift, suggesting an acylation effect or some other modification.

The figure above clearly illustrates a shift in abundance of MSN5 (black ellipse) toward the left, to MSN14, by PFDA treatment and confirms a PFDA effect previously observed [29]. Not only is the abundance of MSN5 significantly reduced and MSN14 increased by PFDA treatment, but MSN18, 1536, and 1537 are more abundant in the PFDA group as well. The effect depicted above is illustrated on the next page in Figure 11 for all patterns and all treatments. This illustration explicitly shows that the charge shift is limited to perfluorocarboxylic acid exposures and is not observed when rats are exposed to either clofibrate or DEHP. Group means shown in Figure 12 for the individual effects in the montage above conclusively demonstrate the specific PFDA-induced shift in protein abundance. The cause of this charge variation is not yet known. Previous studies of halothane hepatitis [39,40] have demonstrated

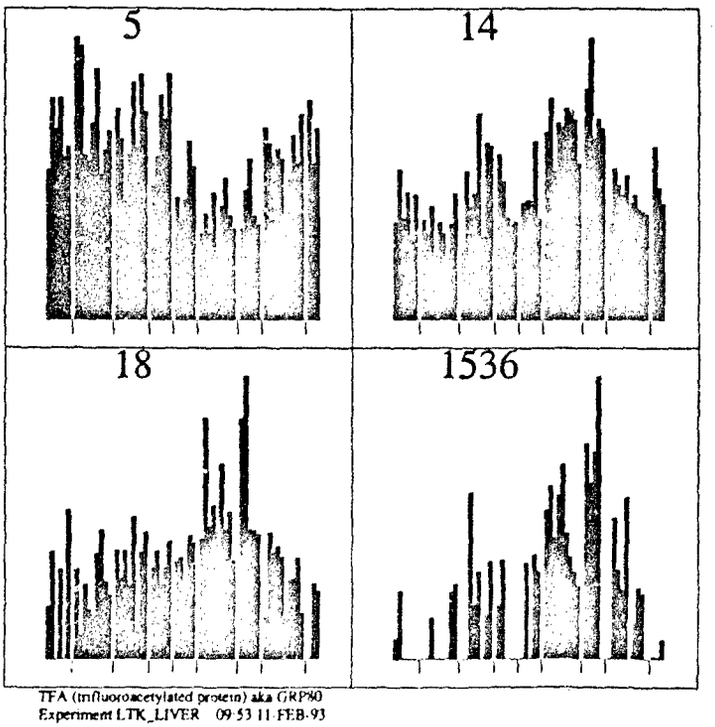

Figure 11. Bar graphs showing the abundance of the heterogeneous forms of TFA protein (MSN5,14,18,1536) in rat liver whole homogenates of different treatment groups. Each bar represents the abundance of that protein in each animal's 2D pattern with gaps separating the different groups (group 1 is ad lib control; group 2 is pair-fed; group 3 is PFOA-treated, group 4 is PFDA 2mg/kg; group 5 PFDA 20mg/kg; group 6 PFDA 50mg/kg 8da; group 7 PFDA 50mg/kg 30da; group 8 clofibrate; and group 9 DEHP treated. Missing bars indicate the absence of a protein in an animal.

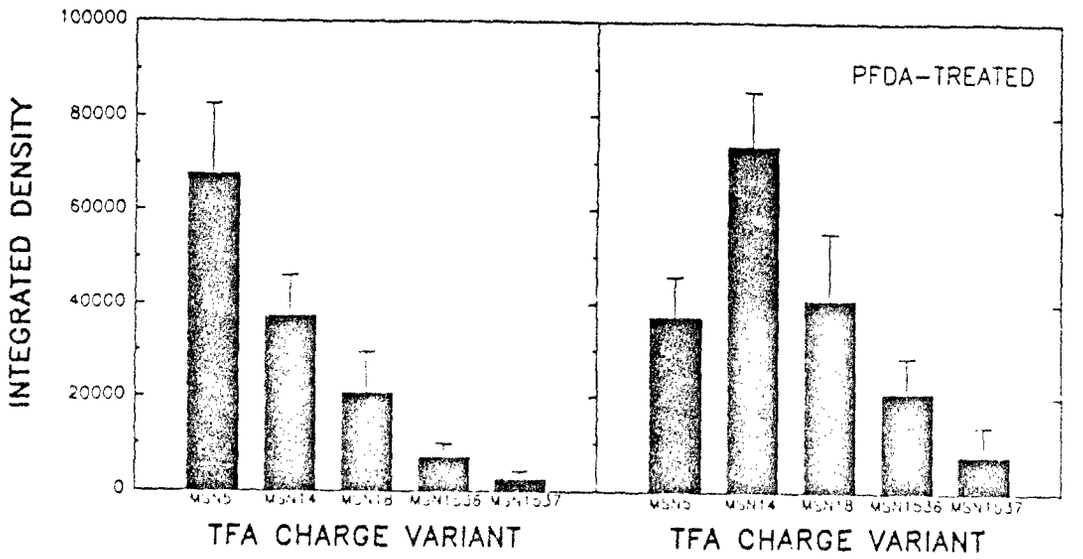

Figure 12. Bar graph showing the effect of PFDA treatment on the abundance of the various TFA protein charge forms. The graph on the left illustrates means ± SE for the control group. The graph on the right illustrates means ± SE for the PFDA treated group. The controls exhibit a progressive decline in abundance form the native MSN5 form to MSN1537 (which was present in only 2 control animals). PFDA causes a dramatic shift in abundance to more acidic forms suggesting acylation, conjugation or some other post-translational modification unique to PFDA treatment.

the trifluoroacetylation of a 76 kDa protein in the endoplasmic reticulum (TFA-76). That MSN14 cross-reacts with the antisera formed against TFA-76 [32] from those studies suggests this protein may be acylated by a metabolite of PFDA and thereby acquire some structural similarity to the trifluoroacyl conjugate. On the other hand, the charge shift observed may be the result of increased glycosylation of the native form in PFDA treated livers. To answer this question, we are currently attempting to synthesize PFDA-protein conjugates to generate antibodies. We are also interested in the synthesis of ^{14}C-labelled PFDA to investigate putative conjugation by autoradiography.

SUMMARY AND CONCLUSIONS

Regarding the original objectives stated in the project proposal, each was achieved and in some cases exceeded. State-of-the-art 2D electrophoretic technology and computerized image analysis were successfully integrated into our toxicological approach. A rat liver whole homogenate master pattern was generated and is currently being compared to a rat liver database under development elsewhere [13]. Over 1,400 proteins have been resolved reproducibly and 64 protein spots in the F344LIVER master pattern number system have been identified (Table 1). Of the 64 proteins identified, several have been studied with regard to perfluorocarboxylic acid effects and the results *1)* confirm previous independent observations regarding PFOA, PFDA, and clofibrate hepatotoxicity and *2)* reveal novel PFDA-effects that suggest a complex toxic mechanism. Although PFDA's specific mechanism and peroxisome proliferative mechanisms in general have not been elucidated from these data, this study has confirmed our expectation that high-resolution 2D electrophoresis in combination with image analysis is indeed a powerful tool in the assessment of xenobiotic effects. As more protein are identified in our database of rat liver 2D patterns and those of others, it will be possible to assess enzyme induction and protein-bound metabolites of toxicants and to explore cellular metabolic pathways associated with specific intoxications (*i.e.* peroxisomal β-oxidation).

This project has satisfied established criteria (13) for systematic use of 2-D electrophoresis in toxicology: *1)* a useful range of known effects produces detectable changes at the molecular level, *2)* that there is sufficient specificity associated with molecular effects to differentiate various classes of mechanisms, and *3)* that there is some basis for expecting that the molecular changes can be interpreted in a way that helps illuminate not only the details, but also the possible significance, of the events observed.

BIBLIOGRAPHY

1. O'Farrell, P. (1975) *J. Biol. Chem.* 250:40047-4021.
2. Anderson, N.G. and Anderson, N.L. (1978) *Anal. Biochem.* 85:331-340.
3. Anderson, N.L. and Anderson, N.G. (1978) *Anal. Biochem.* 85:341-354.
4. Anderson, L. and Anderson, N. (1984) *Clin. Chem.* 30:1898-1905
5. Anderson, N.L., Esquer-Blasco, R., Hofmann, J.P. and Anderson, N.G. *Electrophoresis* 12:907-930, 1991.
6. Vlasuk, G.P. *et al.* (1982) *Biochem.* 21:6288-6292
7. Jellum, E., Karasek, F.W., and Thorsrud, A.K. (1983) *Anal. Chem.* 55:2340-2344.
8. Watanabe, T., Lalwani, N.D. and Reddy, J.K. (1985) *Biochem J.* 227:767-775.
9. Anderson N.L. *et al.* (1986) *Electrophoresis* 7:44-48.
10. Anderson, N.L. *et al.* (1987) *Fundam. Appl. Toxicol.* 8:39-50.
11. Wirth, P.J. and Vesterberg, O. (1988) *Electrophoresis* 9:47-53.
12. Witzmann, F., Bale, S. and London, S. (1990) *In Vitro Toxicol.* 3:205-217.
13. Anderson, N.L. (1990) In: *New Horizons in Molecular Toxicology*, Ed. G.S. Probst, FASEB, Bethesda, MD, pp. 65-71.
14. Witzmann, F.A. and Parker, D.N. (1991) *Toxicology Letters* 57:29-36.
15. Anderson, N.L. *et al.* (1992) *Fundam. Appl. Toxicol.* 18:570-580.
16. Andersen, M.E., Baskin, G. and Rogers, A.M. *The Toxicologist* 1:16, 1981.
17. Olson, C.T. and Andersen, M.E. *Toxicol. Appl. Pharmacol.* 70:362-372, 1983.
18. Harrison, E.H., Lane, J.S., Luking, S., VanRafelgehm, M.J. and Andersen, M.E. *Lipids* 23:115-119, 1988
19. Ikeda, T., Aiba, K., Fukuda, K. and Tanaka, M. *J. Biochem.* 98:475-482, 1985.
20. VanRafelgehm, M.J., Mattie, D.R., Bruner, R.H., and Andersen, M.E. *Fund. Appl. Toxicol.* 9:522-540, 1987.
21. George, M.E. and Andersen, M.E. *Toxicol. Appl. Pharmacol.* 85:169-180, 1986.
22. Shindo, Y., Osumi, T., and Hasimoto, T. *Biochem. Pharmacol.* 27:2683-2688, 1978.
23. Osmundsen, H. in *"Peroxisomes and Glyoxysomes", Annal. NY Acad. Sci.* 386:13-18, 1982. Eds. H. Kindl and P.B. Lazarow.
24. Gibson, G.G., Orton, T.C. and Tamburini, P.P. *Biochem. J.* 203:161-168, 1982.
25. Sharma, R., Lake, B.G., Gibson, G.G. *Biochem. Pharmacol.* 37:1203-1206, 1988.
26. Witzmann, F., DelRaso, N., and George, M. *The Toxicologist* 10:251, 1990.
27. Witzmann, F.A. (1990) *Proceedings, Society of Environmental Toxicology and Chemistry Annual Meeting* p. 177.
28. Witzmann, F.A. and Parker, D.N. (1990) *Proceedings, ISSX North American Meeting*
29. Witzmann, F.A. and Parker, D.N. (1991) In: *2D PAGE '91: Proceedings of the International Meeting on Two-dimensional Electrophoresis*, M.J. Dunn, Ed., Zebra Printing, Middlesex UK, pp. 236-237, 1991.
30. Witzmann, F.A., Jarnot, B.M. and Parker, D.N. (1991) *Electrophoresis* 12:687-688.
31. Witzmann, F.A., Parker, D.N. and Jarnot, B.M. (1991) *The Toxicologist* 11:348.
32. Witzmann, F.A. (1991) *Clin. Chem.* 37:1096.
33. Witzmann, F.A., Parker, D.N. and Jarnot, (1992) *Toxicologist* 12:417.
34. Witzmann, F.A., George, M.E., Jarnot, B.M. and Parker, D.N. (1992) *Proceedings, ISSX North American Meeting.*
35. Anderson, N.L. (1988) *Two-dimensional Electrophoresis: Operation of the ISO-DALT® System*, Large Scale Biology Press, Washington DC, pp. 3-15, 142.

36. Chappall, J.B. and Hansford, R.G., in: Birnie, G.D. (Ed.) (1972) *Subcellular Components*, Butterworths, London, pp. 77-91.
37. Neuhoff, V., Arold, N., Taube, D., and Ehrhardt, W. (1988) *Electrophoresis* 9:255-262.
38. O'Farrell, P.Z., Goodman, H.M., and O'Farrell, P.H., (1977) *Cell* 12:1133-1142.
39. Pumford, N.R., Pohl, L.R. et al. *The Toxicologist* 11:1031-1032, 1991.
40. Kenna, J.G., Satoh, H., Christ, D.D., and Pohl, L.R. (1988) *J. Pharmacol. Exp. Ther.* 245:1103-1109.

Publications resulting from this effort:

Hepatic protein alterations following perfluorodecanoic acid exposure in rats. Witzmann, F.A. and Parker, D.N. **Toxicology Letters** 57:29-36, 1991.

Dodecyl maltoside detergent improves the resolution of hepatic membrane proteins on two-dimensional gels. Witzmann, F.A., Jarnot, B.J., and Parker, D.N. **Electrophoresis** 12:687-688, 1991.

Hepatotoxicity of perfluorinated compounds in male rats: 2D-PAGE analysis. Witzmann, F.A. and Parker, D.N. In: **2-D PAGE '91: Proceedings of the International Meeting on Two-Dimensional Electrophoresis**, M.J. Dunn, Ed. 1991, Zebra Printing, Middlesex UK, pp. 236-237.

Papers presented at scientific meetings:

Two-dimensional electrophoretic analysis of PFDA hepatotoxicity. Witzmann, F.A., DelRaso, N. and George, M. at the 29th Annual Meeting of the Society of Toxicology, February 12-16, 1990 in Miami Beach FL. Published as an abstract in **The Toxicologist** 10:251, 1990.

Induction of cytochrome P452 in liver cell fractions by perfluoro-n-decanoic acid: an electrophoretic analysis. Witzmann, F.A. and D.N. Parker. Presented at the North American Meeting of the International Society for the Study of Xenobiotics, October 1990 in San Diego CA.

Two-dimensional protein electrophoresis: Hepatotoxic applications. Witzmann, F.A. Presented at the Society of Environmental Toxicology and Chemistry Annual Meeting, November 1990 in Alexandria VA.

Induction of an 80kDa protein in rat liver homogenates and cell fractions by perfluoro-n-decanoic acid. Witzmann, F.A. and Parker, D.N. Presented at the 30th Annual Meeting of the Society of Toxicology, February 25-March 1, 1991 in Dallas TX.

Hepatotoxicity of perfluorinated compounds in male rats: 2D-PAGE analysis. Witzmann, F.A. and Parker, D.N. Presented at the International 2D-PAGE Conference, July 16-19, 1991 in London England.

Perfluoro-n-decanoic acid toxicity in the rat liver: Two-dimensional electrophoretic analysis. Witzmann, F.A. Presented as an invited selected topics lecture in *Molecular Pathology: Applications to the Study of Xenobiotic Effects in Animal Testing* at the 43rd National Meeting of the American Association for Clinical Chemistry, July 28-August 1, 1991 in Washington DC; published as an abstract in **Clinical Chemistry** 37:1096, 1991.

Perfluorocarboxylic acid intoxication increases ß-oxidative enzyme content of hepatic mitochondrial fractions in rodents. Witzmann, F.A., Jarnot, B.M., and Parker, D.N. Presented at the 31st Annual Meeting of the Society of Toxicology, February 23-27, 1992 in Seattle WA.

Hepatic, renal, and testicular gene product regulation by perfluorocarboxylic acids and clofibrate: Two-dimensional protein mapping and pattern recognition. Witzmann, F.A., George, M.E., Jarnot, B.M., and Parker, D.N. Presented at the Fourth North American ISSX Meeting, November 2-6, 1992 in Bal Harbour FL.